# Supplementary Information

## TMEM135 Links Peroxisomes to the Regulation of Brown Fat Mitochondrial Fission and Energy Homeostasis

Donghua Hu, Min Tan[1], Dongliang Lu, Brian Kleiboeker, Xuejing Liu, Hongsuk Park, Alexxai V. Kravitz, Kooresh I. Shoghi, Yu-Hua Tseng, Babak Razani, Akihiro Ikeda, and Irfan J. Lodhi

**Supplementary information includes seven Supplementary Figures and one Supplementary Table.**

**Supplementary Fig. 1.** Effect of Pex16 deficiency on mitochondrial respiration and mitophagy in mouse brown adipocytes.

**Supplementary Fig. 2.** TMEM135 is present in peroxisomes and mitochondria.

**Supplementary Fig. 3.** TMEM135 gene expression increases during BAT SVF cell differentiation and after NE treatment.

**Supplementary Fig.4.** Metabolic phenotyping of *Tmem135-AKO* mice.

**Supplementary Fig. 5.** Metabolic phenotyping of *Tmem135*$^{TG}$ mice.

**Supplementary Fig. 6.** Overexpression of TMEM135 in *Pex16-AKO* mice rescues cold tolerance and mtDNA copy number.

**Supplementary Fig. 7.** Gene expression analysis and effect of TMEM135 KD on mitochondrial morphology in different cell types**.**

**Supplementary Table 1.** Oligonucleotide sequences

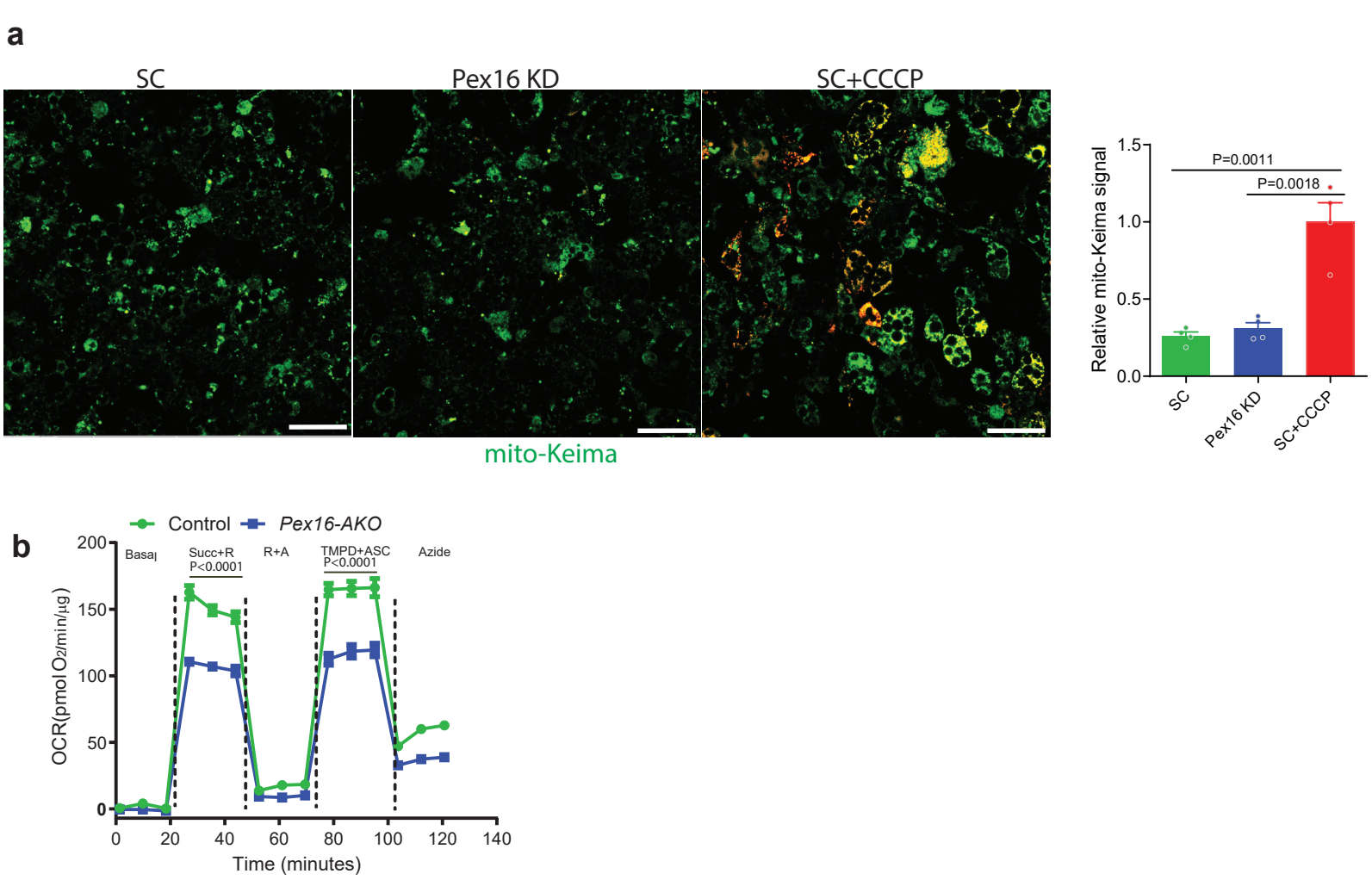


**Supplementary Fig. 1. Effect of Pex16 deficiency on mitochondrial respiration and mitophagy in mouse brown adipocytes.** (**a**) Confocal imaging of mitophagy using mito-Keima in brown adipocytes treated with scrambled (SC) (n=4) or Pex16 shRNA (n=4). Carbonyl cyanide m-chlorophenylhydrazone (CCCP) was used as a positive control (n=4) to induce mitophagy. Plot shows quantification of mito-Keima signal. Scale bar: 50 µm. (**b**) OCR measured using a Seahorse XF24 Extracellular Flux Analyzer in frozen BAT isolated from control (n=5) and Pex16-AKO (n=5) mice subjected to 3 day cold exposure. Succ+R, Succinate + Rotenone; R+A, Rotenone + antimycin A; TMPD+ASC, N,N,N',N'-tetramethyl-p-phenylenediamine + Ascorbic acid. Data are presented as mean ± SEM; statistical significance was determined by Student's t test (**a**) or 2-way ANOVA with Bonferroni's post hoc test (**b**).

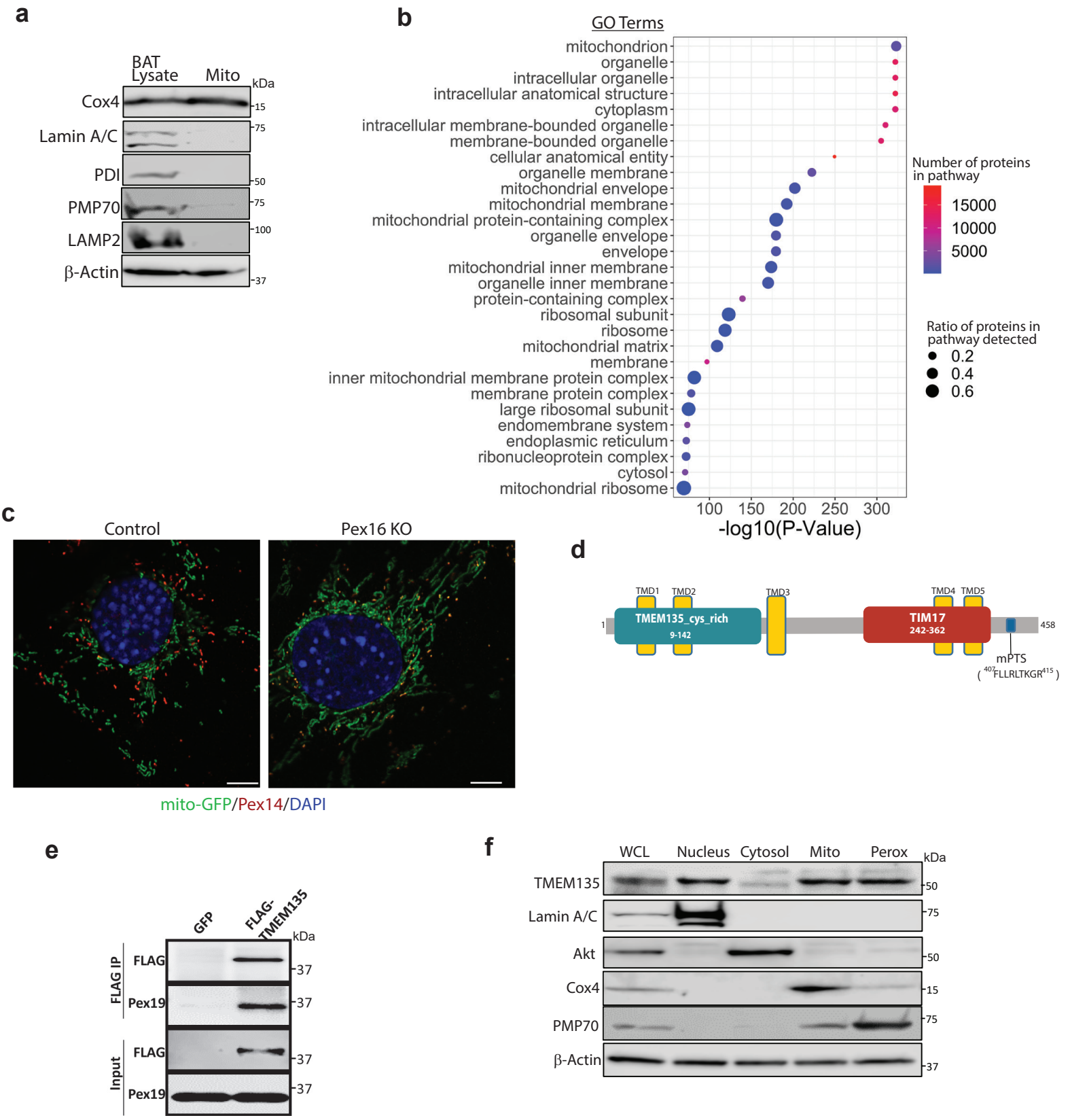


**Supplementary Fig. 2. TMEM135 is present in peroxisomes and mitochondria.**
(**a**) Western blot analysis of whole BAT lysate and mitochondrial fraction from brown adipose of wild-type C57BL/6J mice. (**b**) Gene Ontology (GO) terms (cellular component ontology) for unchanged proteins identified by mass spectrometry-based proteomics in mitochondria isolated from BAT of control and Pex16-AKO mice. (**c**) Immunofluorescence analysis in control and Pex16-AKO brown adipocytes expressing mito-GFP stained with an antibody against Pex14. Scale bar: 5 μm. (**d**) A model of TMEM135 domain architecture showing that the protein contains an N-terminal TMEM135_Cys_rich domain and a C-terminal TIM17 domain. (**e**) Co-immunoprecipitation of endogenous Pex19 with FLAG-TMEM135 in HEK293 cells. (**f**) Western blot analysis of TMEM135 and organelle markers in whole cell lysates (WCL) and various subcellular fractions of differentiated brown pre-adipocytes from the wild-type C57BL/6J mice.

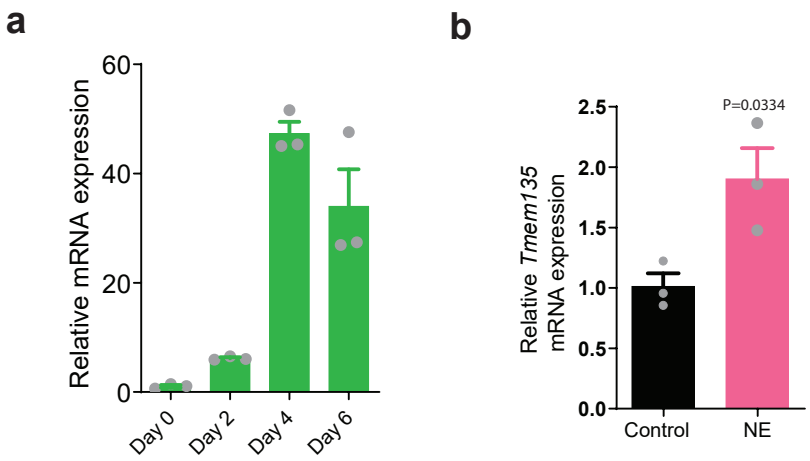


**Supplementary Fig. 3. TMEM135 gene expression increases during BAT SVF cell differentiation and after NE treatment.** (**a**) qPCR analysis of *Tmem135* expression during adipogenesis in mouse BAT SVF cells; n=3. (**b**) qPCR analysis of *Tmem135* expression in brown adipocytes treated with NE (1μM) for 2 hours; n=3. Data are presented as mean ± SEM; statistical significance was determined by two-tailed unpaired Student's t test (**b**).

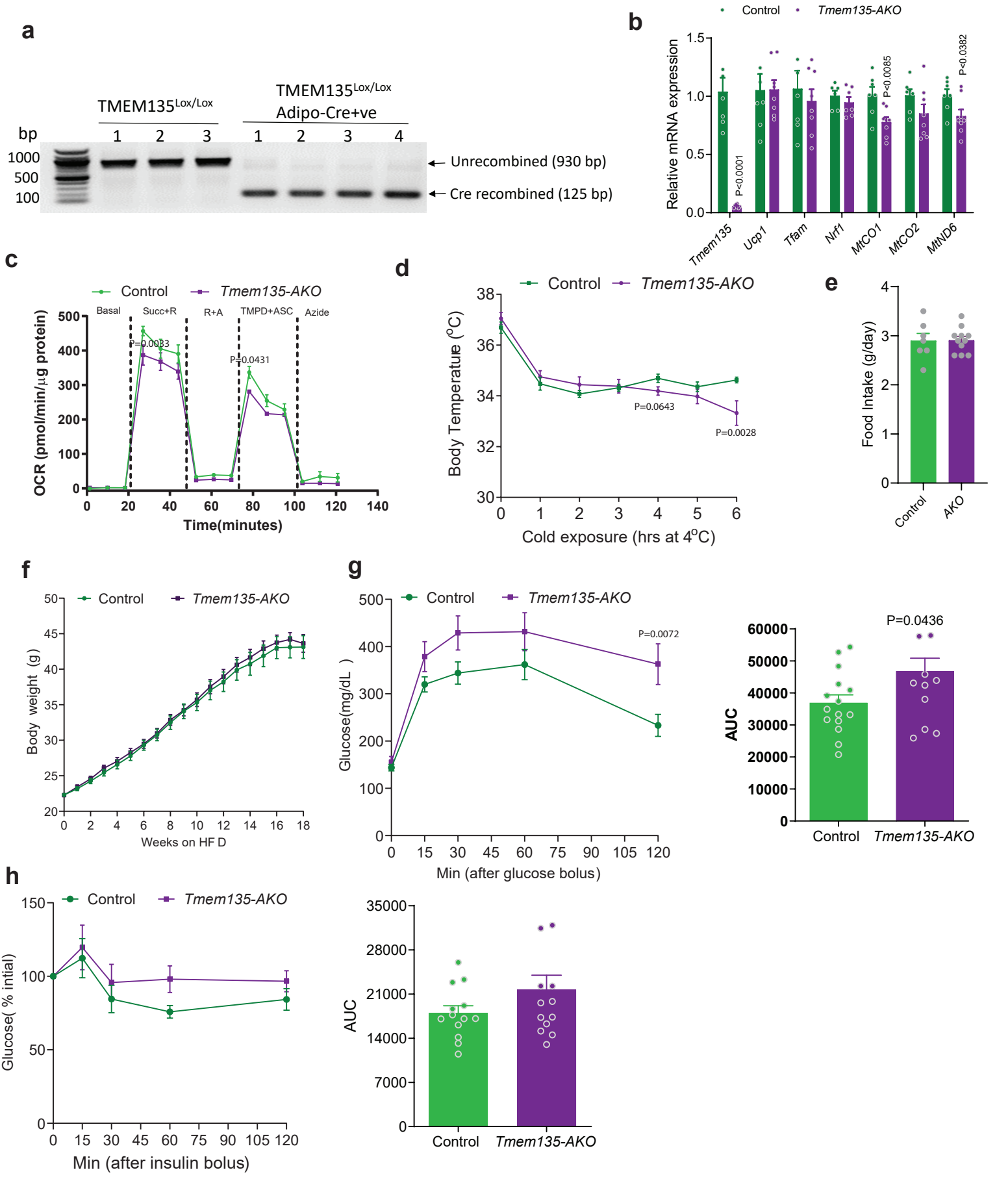


**Supplementary Fig.4. Metabolic phenotyping of *Tmem135-AKO* mice.**
(**a**) Confirmation of Cre-mediated recombination of the floxed alleles in *Tmem135-AKO* mice. (**b**) qPCR analysis of mitochondria-encoded genes in control (n=7) and *Tmem135-AKO* (n=8) mice. (**c**) OCR measured using a Seahorse XF24 Extracellular Flux Analyzer in frozen BAT isolated from control (n=5) and *Tmem135-AKO* (n=5) mice subjected to 7 day cold exposure; Succ+R, Succinate + Rotenone; R+A, Rotenone + antimycin A; TMPD+ASC, N,N,N',N'-tetramethyl-p-phenylenediamine + Ascorbic acid.

(**d**) Body temperature of male *Tmem135-AKO* (n=10) and control (n=17) mice subjected to a 6-hour cold challenge. (**e**) Food intake of female HFD-fed *Tmem135-AKO* (n=11) and control (n=7) mice. (**f**) Body weight of male HFD-fed *Tmem135-AKO* (n=15) and control (n=16) mice. (**g**) Glucose tolerance testing and AUC in male HFD-fed *Tmem135-AKO* (n=13) and control (n=15) mice. (**h**) Insulin tolerance testing and AUC in male HFD-fed *Tmem135-AKO* (n=13) and control (n=13) mice. Data are presented as mean ± SEM; statistical significance was determined by two-tailed unpaired Student's t test (**b, d, e, f, g** and **h**) or 2-way ANOVA with Bonferroni's post hoc test (**c, g,** and **h**).

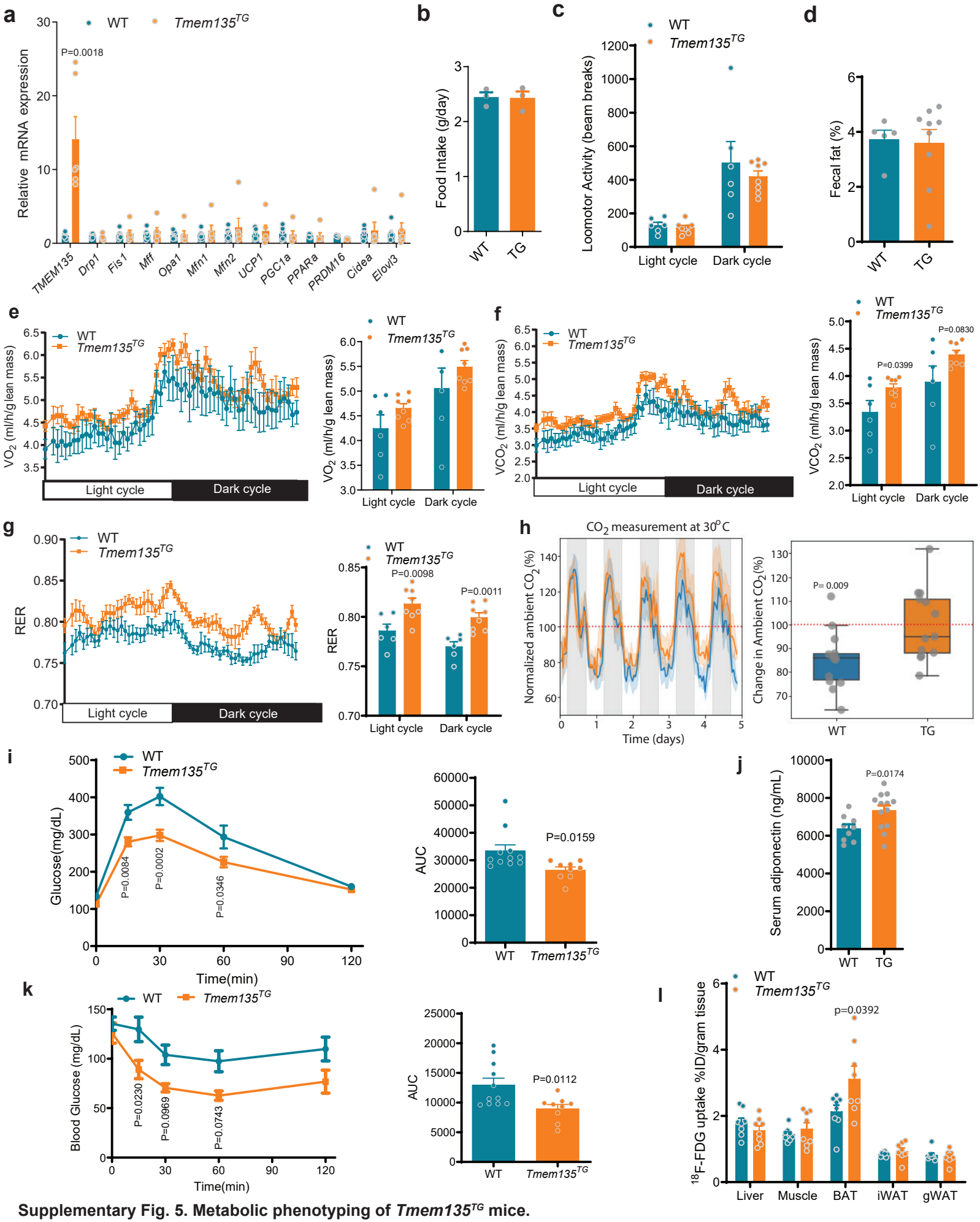


**Supplementary Fig. 5. Metabolic phenotyping of *Tmem135*$^{TG}$ mice.**
(**a**) qPCR analysis of mitochondrial dynamics and thermogenic genes in BAT of *Tmem135*$^{TG}$ (n=6) and WT (n=6) mice. (**b**) Food

intake of male *Tmem135*$^{TG}$ (n=3) and WT (n=3) mice fed a high fat diet. (**c**) Locomotor activity in male HFD-fed *Tmem135*$^{TG}$ (n=8) and WT (n=6) mice. (**d**) Fecal fat of male HFD-fed *Tmem135*$^{TG}$ mice fed a high fat diet. These mice were placed in metabolic cages for 48 hours with 12-hour light/dark cycles; WT n=5; Tmem135$^{TG}$ n=9. (**e**)-(**g**) $VO_2$, $VCO_2$, and respiratory exchange ratio (RER) of *Tmem135*$^{TG}$ (n=8) and WT (n=6) mice fed a HFD for 4 weeks, prior to significant difference in body weight. (**h**) Change of carbon dioxide generation using an in-cage $CO_2$ monitor in *Tmem135*$^{TG}$ (n=14) and WT (n=13) mice maintained at thermoneutrality. (**i**) Glucose tolerance testing and AUC of female HFD-fed *Tmem135*$^{TG}$ (n=9) and WT (n=11) mice. (**j**) Fasting serum adiponectin of male HFD-fed *Tmem135*$^{TG}$ (n=13) and WT (n=9) mice. (**k**) Insulin tolerance testing and AUC of female HFD-fed Tmem135$^{TG}$ (n=9) and WT (n=11) mice. (**l**) Quantification of $^{18}$F-FDG uptake in indicated tissues from male Tmem135$^{TG}$ (n=8) and WT (n=8) mice fed with a high fat diet for 14 weeks. Data are presented as mean ± SEM; statistical significance was determined by two-tailed unpaired Student's t test (**a-d, h, l, j, k** and **l**) or 2-way ANOVA with Tukey's honest significant difference post hoc test (**e-g**) or Bonferroni's post hoc test (**i** and **k**).

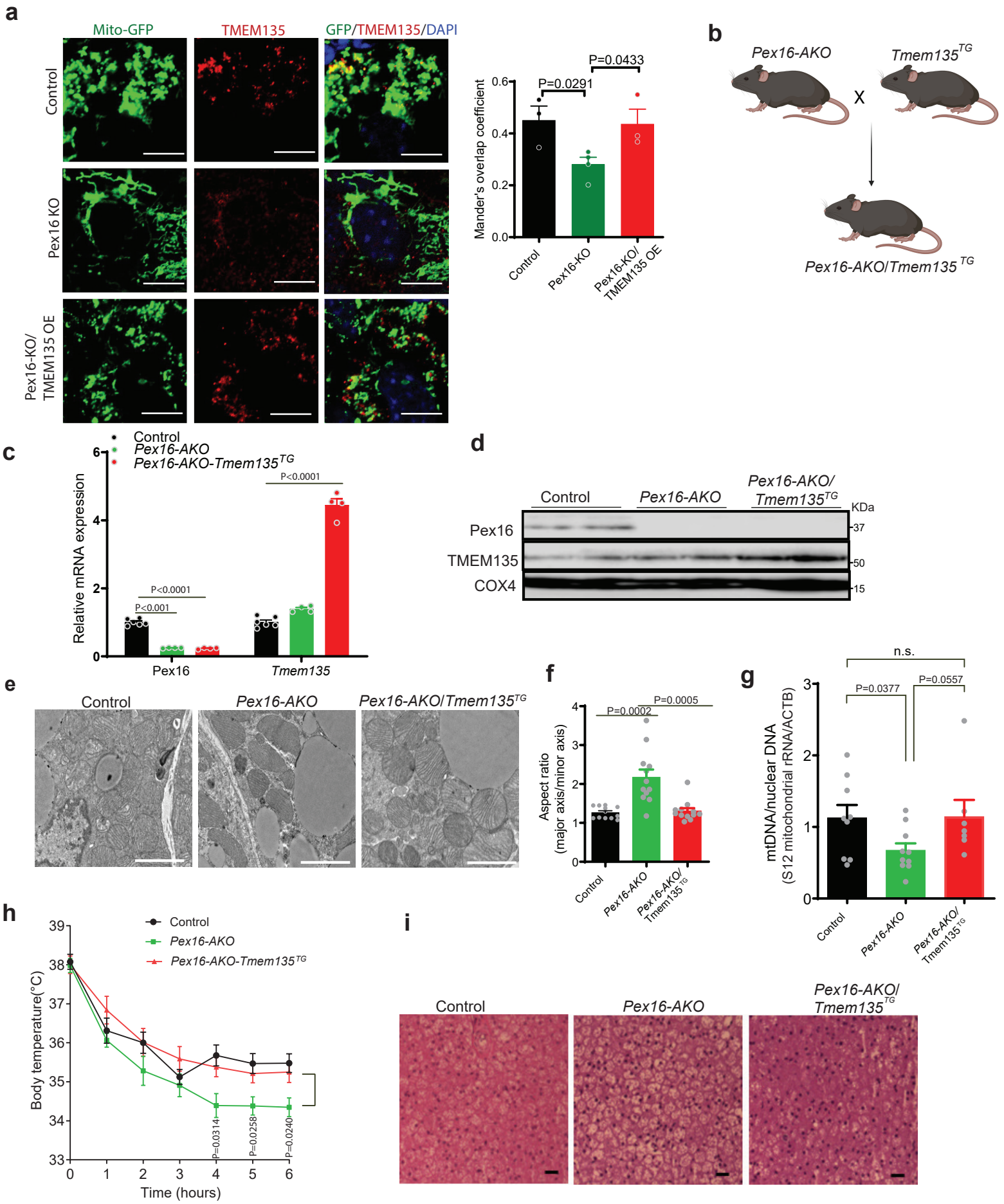


**Supplementary Fig. 6. Overexpression of TMEM135 in *Pex16-AKO* mice rescues cold tolerance and mtDNA copy number.** (**a**) Immunofluorescence analysis in control (*Pex16*$^{lox/lox}$), Pex16 KO (*Pex16*$^{lox/lox}$; adipo-Cre positive) and Tmem135 overexpressing Pex16 KO (Pex16 KO/TMEM135 OE) brown adipocytes stably expressing mito-GFP. Quantification of the colocalization using ImageJ. Scale bar: 10 μm. The images are representative of three independent experiments and the quantification is based on a

total of 27 control, 50 Pex16-KO cells, and 26 Pex16 KO-Tmem135 OE cells. (**b**) Simplified breeding scheme of *Pex16-AKO/Tmem135*$^{TG}$ double mutant mice. Created with BioRender.com. (**c**) and (**d**) qPCR (control n=6; *Pex16-AKO* n=4; *Pex16-AKO*/*Tmem135*$^{TG}$ n= 4) and Western blot (n=2 for each group) analysis of Pex16 and TMEM135 in *Pex16-AKO*/*Tmem135*$^{TG}$ double mutant mice. (**e**) TEM analysis of BAT from control, *Pex16-AKO* and *Pex16-AKO*/*Tmem135*$^{TG}$ double mutant mice subjected to 3 day cold exposure. Scale bar: 1 µm. (**f**) Aspect ratio (ratio of major axis length to minor axis length) measured in BAT mitochondria. Data are based on 12 mitochondria per condition. (**g**) mtDNA copy number normalized to nuclear DNA in control, *Pex16-AKO* and *Pex16-AKO*/*Tmem135*$^{TG}$ double mutant mice subjected to 3 day cold exposure; control n=9; *Pex16-AKO* n=10; *Pex16-AKO*/*Tmem135*$^{TG}$ n=7. (**h**) Body temperature of control, *Pex16-AKO* and *Pex16-AKO*/*Tmem135*$^{TG}$ double mutant mice subjected a 6-hour cold challenge; control n=9; *Pex16-AKO* n=11; *Pex16-AKO*/*Tmem135*$^{TG}$ n= 8. (**i**) H&E staining of control, *Pex16-AKO* and *Pex16-AKO*/*Tmem135*$^{TG}$ double mutant mice subjected to 3 days cold exposure. The images are representative of 3 mice per genotype. Scale bar: 50 µm. Data are presented as mean ± SEM; statistical significance was determined by two-tailed unpaired Student's t test (**a, c, f, g,** and **h**).

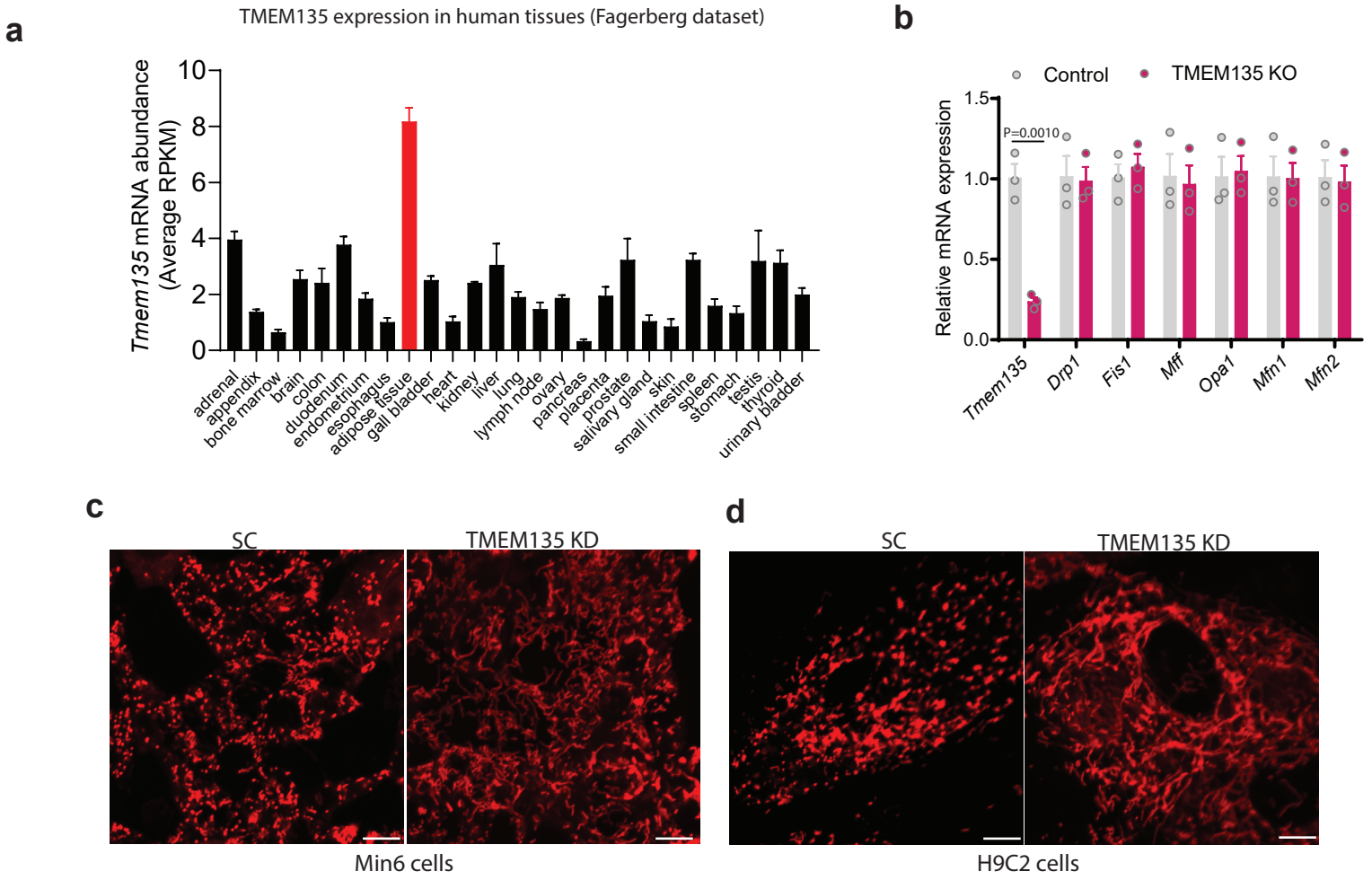


**Supplementary Fig. 7. Gene expression analysis and effect of TMEM135 KD on mitochondrial morphology in different cell types.**
(**a**) *Tmem135* gene expression in major human tissues, based on publicly available data (Fagerberg et al. [Ref 47]). (**b**) qPCR analysis of mitochondrial dynamics genes in control (n=3) and TMEM135 KO (n=3) human brown adipocytes. (**c**) Mitochondrial morphology of in Min6 mouse insulinoma cells treated with scrambled (SC) or TMEM135 shRNA and stained with TMRE for using confocal microscopy. Scale bar: 10 μm. (**d**) Mitochondrial morphology of in H9C2 rat cardiomyocytes treated with scrambled (SC) or TMEM135 shRNA and stained with TMRE for using confocal microscopy. Scale bar: 10 μm. Data are presented as mean ± SEM; statistical significance was determined by two-tailed unpaired Student's t test (**b**).

Supplementary Table 1. Oligonucleotide sequences.

| Name | Forwad(5'-3') | Reverse (5'-3') |
|---|---|---|
| L-32 | TTC CTG GTC CAC AAT GTC AA | GGC TTT TCG GTT CTT AGA GGA |
| TMEM135 | AGG CTG GAA AGG TTC CCT ATT | CGC CAG TAC CAA ACA CAT CC |
| Pex16 | CCG TTC TAT GAC CGC TTC TC | GGA GGG CAA GTA GTC CAT GA |
| PMP70 | TCT GCC TAC TCC ATA AGC GG | CAC CAC AGC TCG CTC TTT CT |
| Drp1 | AGA TCG TCG TAG TGG GAA CG | AGA ATG AGA GGT CTC CGG GT |
| Fis1 | ATT TGA ATA TGC CTG GTG CC | CAT AGT CCC GCT GTT CCT CT |
| Opa1 | TGG AAA ATG GTT CGA GAG TCA G | CAT TCC GTC TCT AGG TTA AAG CG |
| Mff | GGA GTT CCA AAT GCC AGT GTG ATA | TGG ATA AGG TCA AGA TCT GCT GGT |
| Mfn1 | TGA ATA ACC GTT GGG ATG CT | GCT TCC GAC GGA CTT ACA AC |
| Mfn2 | GTC CTG GAC GTC AAA GGG TA | ATT GAT CAC GGT GCT CTT CC |
| UCP1 | TCA GCT GTT CAA AGC ACA CA | GTA CCA AGC TGT GCG ATG TC |
| PGC1α | TGT AGC GAC CAA TCG GAA AT | TGA GGA CCG CTA GCA AGT TT |
| PRDM16 | CAG AGG TGT CAT CCC AGG AG | ACG GAT GTA CTT GAG CCA GC |
| PPARα | AGT TCG GGA ACA AGA CGT TG | CAG TGG GGA GAG AGG ACA GA |
| Cidea | CAGTGATTTAAGAGACGCGG | TCTGCAATCCCATGAATGTC |
| Elovl3 | CTT AAG GCC CTT TTT GGA GG | CCG CGT TCT CAT GTA GGT CT |
| GNPAT | CATGGACGTTCCTAGCTCCT | CCCACTTTTTGAGGTCTTTCG |
| Tfam | CCAAAAAGACCTCGTTCAGC | GACAGATTTTTCCAAGCCTCA |
| Nrf1 | TAGTCCTGTCTGGGGAAACC | CTGGTACATGCTCACAGGGA |
| MtCO1 | TCCTACCACCATCATTTCTCC | CTGATGCTCCTGCATGGG |
| MtCO2 | CATCAAACCGACCAGGGTT | AATTATTGAAGCAGATCAGTTTTCG |
| MtND6 | CCAACATAACTCCAACATCATCA | GTATTGGGGGTGATTATAGAGGTTT |
| Mito-DNA | TTA AGA CAC CTT GCC TAG CCA CAC | CGG TGG CTG GCA CGA AAT T |
| Nucler-DNA | ATG ACG ATA TCG CTG CGC TG | TCA CTT ACC TGG TGC CTA GGG C |
| huL-32 | AAG TTC CTG GTC CAC AAC GTC AA | CAG CTC TTT CCA CGA CTT T |
| huTMEM135 | CTC CTC TGT ACT TGA TTG CAG C | TGA AGC GGA TTG TAG GAT CTC A |
| hDrp1 | CTG CCT CAA ATC GTC GTA GTG | GAG GTC TCC GGG TGA CAA TTC |
| hFis1 | GTC CAA GAG CAC GCA GTT TG | ATG CCT TTA CGG ATG TCA TCA TT |
| hOpa1 | TGT GAG GTC TGC CAG TCT TTA | TGT CCT TAA TTG GGG TCG TTG |
| hMff | ACTG AAG GCA TTA GTC AGC GA | TCC TGC TAC AAC AAT CCT CTC C |
| hMfn1 | TGG CTA AGA AGG CGA TTA CTG C | TCT CCG AGA TAG CAC CTC ACC |
| hMfn2 | CTC TCG ATG CAA CTC TAT CGT C | TCC TGT ACG TGT CTT CAA GGA A |
| huMito-DNA | ACA CAG CAA GAC GAG AAG ACC CTA | TAC TGC TCG GAG GTT GGG TTC T |

| | | |
|---|---|---|
| huNucler-DNA | AAG GGC GCT TTC TCT GCA CA | CAT AGG AAT CCT TCT GAC CCA TGC |